Quantification of Cooperativity between Metal Sites in Dinuclear Transition Metal Complexes Containing the (2-Dimethylamino)-4-(2-pyrimidinyl)pyrimidine Ligand

Tatjana Wall,[a, b] Marko Leist,[b] Fabian Dietrich,[a, b, c] Werner R. Thiel,*[b] and Markus Gerhards+*[a, b]

A concept for the quantification of cooperative effects in transition-metal complexes is presented. It is demonstrated for a series of novel N,N- (mononuclear) and C,N-coordinated homo- and heterometallic binuclear complexes based on the (2-dimethylamino)-4-(2-pyrimidinyl)pyrimidine ligand, which are accessible by applying roll-over cyclometallation. These iridium-, platinum-, and palladium-containing compounds are investigated with respect to their absorption and fluorescence spectra. The cooperative effects in the electronic absorptions, i.e., the energetic shifts between mononuclear and dinuclear complexes, and free ligands are analyzed on the basis of the lowest energy π-π* transitions and compared to calculated data, obtained from TD-DFT calculations. Furthermore the corresponding fluorescence spectra are presented and analyzed with respect to the concept of cooperativity.

Introduction

The term cooperative effect is widely used in chemistry to describe a benefit resulting from the combination of several reaction partners under the premise that the overall effect is greater than the sum of the individual effects. This concept is used in biochemistry and in catalytic processes, where, for example, the combination of several transition metals leads to an increase in product yield compared to monometallic species.[1,2] The interaction of metal sites in polynuclear complexes has been studied for a number of transition metals, particularly in the context of cooperative effects, where the interaction of multiple metals creates special features that are unknown for monometallic complexes.[3] One way to quantify cooperativity in chemical reactions is to consider chemical equilibrium constants.[4]

A general definition of cooperativity is given by theoretical chemists: "When the total energy or another physical property of a many-body system is determined by more than pairwise contributions of its components, cooperativity or anti-cooperativity is involved.".[5] Following this definition, we want to introduce a simple and straightforward method for quantifying cooperativity. One way to determine the cooperative effects is to directly consider the interactions between individual bodies in a system.[6] In contrast to the consideration of three-body terms as shown for the trinuclear transition metal complexes $[M_3\{Si(mt^{Me})_3\}_2]$ (M = Pd, Pt; mt^{Me} = methimazole),[7,8,9] we focus in our model systems on binuclear complexes of a bidentate ligand and compare their properties with their mononuclear counterparts. We assume that this model can be used for a broader variety of metal complexes than a pure focus on three-body terms.

Concepts

Cooperativity

Following the above mentioned definition, we compare properties of the binuclear complexes with the properties of the corresponding mononuclear complexes. However, for most properties it is not sufficient to consider only the metals in the complexes but also the interaction of the metals with the ligand. Hence, the properties of the pure ligand also have to be taken into account. With respect to cooperativity, the following question arises: Is it possible to predict a certain property P of a binuclear complex (AB) from the knowledge of the properties of two corresponding mononuclear complexes (A and B) and of the ligand?

[a] T. Wall, Dr. F. Dietrich, Prof. Dr. M. Gerhards+
Research Center Optimas
TU Kaiserlautern
Erwin-Schrödinger-Str. 52, 67663 Kaiserslautern (Germany)
E-mail: gerhards@chemie.uni-kl.de
[b] T. Wall, Dr. M. Leist, Dr. F. Dietrich, Prof. Dr. W. R. Thiel, Prof. Dr. M. Gerhards+
Fachbereich Chemie
TU Kaiserslautern
Erwin-Schrödinger-Str. 54, 67663 Kaiserslautern (Germany)
E-mail: thiel@chemie.uni-kl.de
[c] Dr. F. Dietrich
Núcleo Milenio MultiMat & Physics Department
Universidad de La Frontera
Francisco Salazar 01145, Temuco (Chile)
[+] Passed away on December 28, 2020.

Supporting information for this article is available on the WWW under https://doi.org/10.1002/cplu.202100049

$$P_{AB} \stackrel{?}{=} P_A + P_B - P_{Ligand} \quad (1)$$

If the answer is yes, there is simple additivity but no cooperativity. If the answer is no, cooperativity (either positive or negative) is observed. It should be mentioned at this point that the terminus cooperativity is not used in a sense of a positive impact or a benefit. This could be the result of cooperativity but has to be considered separately.

Four different cases are possible for a bidentate ligand whose coordination sides differ (Figure 1). The first two lines show the heterobimetallic cooperativity, line three and four the homobimetallic cooperativity.

According to the given definition, in principle every property of the complexes can be used for the analysis of cooperativity. It is likely that different values (positive or negative) for cooperativity will be calculated for different properties.

In studies of cooperativity in catalysis, most of the benefits result from enthalpic cooperativity, i.e. the decrease of an activation barrier in the presence of two or more transition metal centers compared to mono-nuclear complexes.[10] This enthalpic cooperativity may result from polarization or induction effects of the metals interacting with the surrounding environment. A weakening of the bond between the ligand and the first metal induced by the presence of the second metal can lead to a lower catalytic activation barrier. Unfortunately, these effects cannot be observed directly. However, it is possible to observe properties, which are also affected by the effects mentioned above. These properties are e.g. electronic excitation energies, bond lengths and NMR shifts. By measuring these properties and applying our concept, a prediction for the magnitude of cooperativity can be given. This could help to find a promising combination of metals for catalysis.

We want to demonstrate our concept for a series of mono- and binuclear transition metal complexes containing iridium(III), palladium(II) and platinum(II) coordinated to the (2-dimethylamino)-4-(2-pyrimidinyl)pyrimidine ligand. We investigate the electronic transition energy using UV/Vis spectroscopy and TD-DFT calculations.

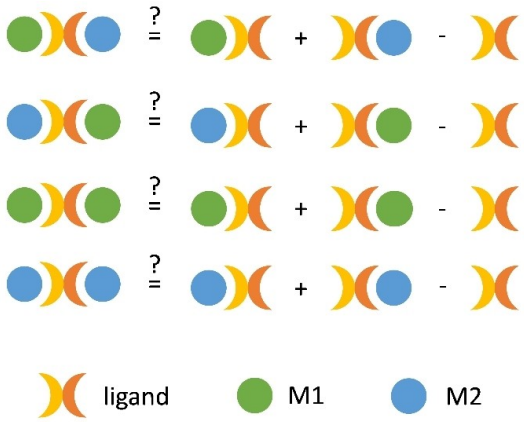

Figure 1. Hetero- and homobimetallic cooperativity.

Synthesis of mono- and binuclear complexes

During the last years, roll-over cyclometallation has turned out to be a versatile strategy for increasing the activity of catalysts.[11–14] However, it is also a highly efficient tool to access bimetallic complexes. For this approach, we designed ligands that create a second chelating donor site by undergoing roll-over cyclometallation, thus enabling the coordination of a second transition metal. To achieve this, we use 2-(2-dialkylaminopyrimidin-4-yl)pyrimidine ligands (Figure 2) which are easily accessible in just a few steps.[15] The dialkylamino group is a prerequisite for the roll-over cyclometallation reaction, since it weakens the N,N'-coordination (N,N' = chelating coordination by two nitrogen donors) by steric interaction and allows the metal to undergo an electrophilic aromatic substitution at the C–H group by increasing the electron density in the upper pyrimidine ring.

In analogy to our already published route to the N,N-coordinated iridium(III) complex **2**,[15] the palladium(II) and platinum(II) complexes **3** and **4** are obtained by treating 2-(2-dimethylaminopyrimidin-4-yl)pyrimidine with appropriate precursor compounds (Figure 3). As expected, complexes **3** and **4** show similar NMR spectra. In the ^{1}H NMR spectra there are two doublets for the protons of the amino-substituted pyrimidine ring and two doublets and one double doublet, appearing as a triplet for the symmetrical pyrimidine ring. Typically, the resonances of the methyl groups are broad at room temperature but split into two sharp singlets by lowering the temperature, which suggests that the rotation around the C–N bond is hindered. From ^{1}H NMR spectra recorded at different temperatures, almost identical rotational barriers could be calculated for the two complexes ($\Delta G_{Rot}^{\neq}$(**3**): 56.7, $\Delta G_{Rot}^{\neq}$(**4**): 55.2 kJ/mol). The cyclometallated iridium(III) complex **5** is obtained in one step starting from 2-(2-dimethylaminopyrimidin-4-yl)pyrimidine and $[Cp^*IrCl_2]_2$ at elevated temperatures and in the presence of a base.[15] Here the ^{1}H NMR spectrum shows as expected only one singlet for the amino-substituted pyrimidine ring and the rotation of the dimethylamino group around the C–N bond is not hindered at room temperature. Roll-over cyclometallation as mentioned above provides a new N,N-coordination site, which then can be used to coordinate palladium(II) and platinum (II) centers, resulting in the formation of the heterobimetallic compounds **6** and **7**.[15] Following this strategy, the N,N coordination of 0.5 equivalents of $[Cp^*IrCl_2]_2$ leads to the cationic homobimetallic complex **8** containing two iridium

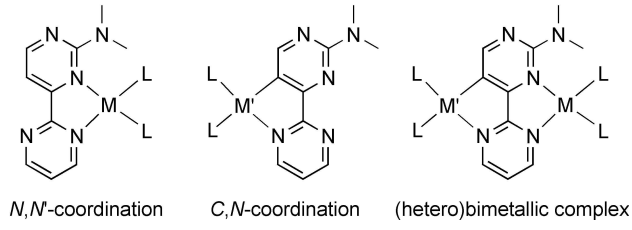

Figure 2. A dipyrimdinyl ligand as a building block to access mono- and dinuclear complexes.

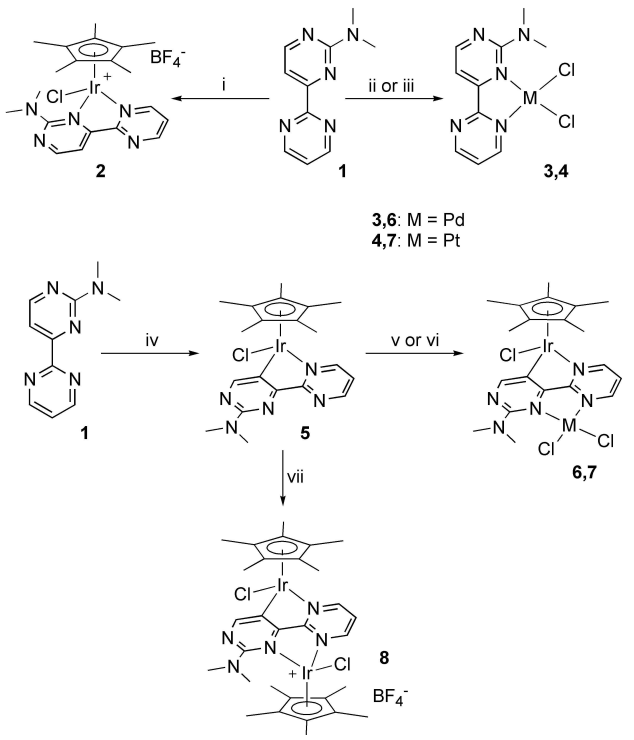

Figure 3. Synthesis of mono- and heterodicnuclear complexes: i) $^1/_2$ $[Cp^*IrCl_2]_2$, $NaBF_4$, CH_2Cl_2, 72 h, r.t.; ii) $PdCl_2$, acetonitrile, 18 h, r.t.; iii) a) $K[(C_2H_4)PtCl_3](H_2O)$, acetone, 96 h, r.t.; iv) $^1/_2$ $[Cp^*IrCl_2]_2$, o-$C_6H_4Cl_2$, 18 h, KOAc, 80 °C; v) $PdCl_2(C_6H_5CN)_2$, acetone, 18 h, r.t.; vi) $K[(C_2H_4)PtCl_3](H_2O)$, acetone, 68 h, r.t.; vii) $^1/_2$ $[Cp^*IrCl_2]_2$, $NaBF_4$, CH_2Cl_2, 72 h, r.t..

(III) sites. Using ^{1}H NMR spectroscopy, a hindered rotation of the dimethylamino group around the C–N bond is observed for compounds **6**, **7** and **8** at room temperature. Steric interaction with adjacent metal sites and their ligand environment raises the rotational barriers resulting in two signals for the NMe_2 group. As expected, a double set of signals is observed for the two Cp* moieties in complex **8**. Due to presence of a cationic charge at one of the iridium(III) sites, the ^{1}H NMR resonance of the Cp* moiety coordinated here is shifted by around 0.40 ppm to lower field compared to the second one.

Following the scheme in Figure 1, the left (yellow) part of the ligand represents the C,N-coordination (C,N = chelating coordination by one carbon and one nitrogen donor), the right (orange) part the N,N-coordination. The synthesized complexes **2**, **3**, **4**, **5**, **6**, **7** and **8** in combination with ligand **1** allow the analysis with respect to the first line with M1 = iridium and M2 = palladium or platinum for two heterometallic cases as well as the third line with M2 = iridium, which represents a homometallic case. The cases of lines two and line four in Figure 1 could not be analyzed, since the C,N-coordination of palladium and platinum was not possible with ligand **1** so far.

Results and Discussion

Absorption and emission spectra (see Figures S13–28 in the Supporting Information) of mono- and binuclear transition metal complexes containing iridium(III) (**2**, **5**–**8**), palladium(II) (**3**, **6**) and platinum(II) (**4**, **7**) as well as spectra of the pure ligand 2-(2-dimethylaminopyrimidin-4-yl)pyrimidine (**1**) were recorded in dichloromethane and chloroform.

The UV/Vis-spectra of the ligand and the transition metal complexes show absorption bands in the spectral region from about 800 to 250 nm (12500 to 40000 cm^{-1}), see Figures S13-28. As an example, the calculated absorption stick spectrum (calculated at the TD-DFT/B3LYP/def2-TZVP level, shown without convolution) of the iridium(III)/palladium(II) complex (**6**) is shown in the Supporting Information (Figure S29). It can be seen that the band with the lowest energy has only the contribution of one transition, whereas for all other bands a mixture of several transitions has to be taken into account. In general, the calculated spectra fit the experimental ones very well.

Ligand **1** has its first electronic excitation at $\tilde{\nu} = 26881\ cm^{-1}$ in CH_2Cl_2 and at $\tilde{\nu} = 26738\ cm^{-1}$ in $CHCl_3$, respectively. The involved orbitals are shown in Figure 4. The HOMO is located on the (2-dimethylaminopyrimidin-4-yl) ring, while the LUMO is delocalized over both heteroaromatic rings. This indicates that the excitation has a π-π^* character accompanied with an intra-ligand charge transfer.

For all complexes, we were looking for similar electronic transitions (Figures S30–37). Adding a metal changes the order of the orbitals – the highest occupied π-orbital of the ligand becomes the HOMO-1 (except for **2** and **8**). Furthermore, this orbital shows a contribution of a metal centered orbital. Since there is an additional node plane between the ligand and the metal, an increase in energy is expected. The LUMO is not affected by the coordination of the metal, since it is still centered on the ligand delocalized over both rings. Consequently, the electronic transitions, we pay attention to, are those from HOMO-1 to LUMO for **3**–**7** and from HOMO to LUMO for **1**, **2** and **8**.

The combination of iridium(III), palladium(II) and platinum(II) shown in Figure 3 yields three series of complexes for the methodology introduced in Figure 1, which are discussed below. The evaluation of the UV/Vis spectra showed for all metal complexes a solvent-dependent and in comparison to

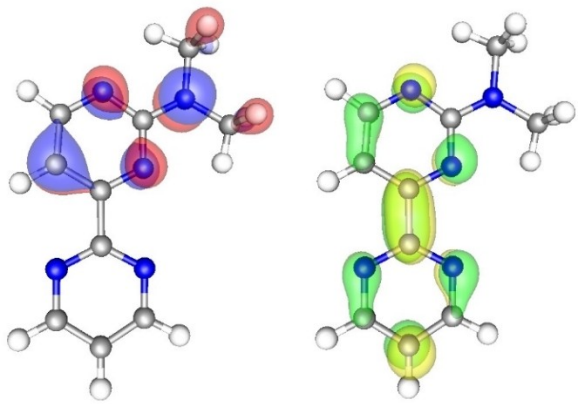

Figure 4. Calculated electron densities of the HOMO (left) and the LUMO (right) of **1**.

the free ligand **1** bathochromically shifted π-π* transition (Table 1). This is consistent with the expected increase of the HOMO/HOMO-1 energy and an unaffected LUMO, resulting in a lower transition energy. Metal-induced bathochromic shifts are known for several biaryl complexes, see e.g. for iridium[16] or platinum.[17,18]

In CH_2Cl_2 the following shifts are observed (see Figures S38–45): The N,N-coordination of palladium in complex **3** induces the smallest shift of 38 nm ($-2491\ cm^{-1}$), while the N,N-coordination of platinum(II) in compound **4** induces a shift of 75 nm ($-4510\ cm^{-1}$), followed by the N,N-coordination of iridium(III) in **2** with 81 nm ($-4807\ cm^{-1}$). The largest shift in the series of monometallic complexes is observed for the C,N-coordinated iridium(III) complex **5** with 144 nm ($-7501\ cm^{-1}$). Binuclear complexes show even larger shifts with 175 nm ($-8600\ cm^{-1}$) for the cationic iridium(III)/iridium(III) complex **8**, 203 nm ($-9490\ cm^{-1}$) for the iridium(III)/platinum(II) complex **7** and 195 nm ($-9245\ cm^{-1}$) for the iridium(III)/palladium(II) complex **6**.

In $CHCl_3$ solution, the following shifts were observed (see Figures S46–53): N,N-Coordination of palladium(II) in complex **3** again induces the smallest shift of 65 nm ($-3959\ cm^{-1}$). N,N-Coordination of iridium(III) in compound **2** induces a shift of 78 nm ($-4614\ cm^{-1}$), which is much smaller than the value observed in CH_2Cl_2. The N,N-Coordination of platinum(II) in compound **4** induces a shift of 119 nm ($-6454\ cm^{-1}$). C,N-Coordination of iridium(III) in complex **5** again induces the largest shift of 142 nm ($-7358\ cm^{-1}$), which is comparable to the value measured in CH_2Cl_2 solution. Binuclear complexes show larger shifts of 157 nm ($-7906\ cm^{-1}$) for cationic iridium (III)/iridium(III) complex **8**, 201 nm ($-9347\ cm^{-1}$) for iridium(III)/palladium(II) complex **6** and 211 nm ($-9644\ cm^{-1}$) for the iridium(III)/platinum complex **7**. The difference for the N,N-coordinated complexes results from the different effective nuclear charges of palladium(II) and platinum(II), where the double positive charge is distributed on the bigger Pd^{2+} ion (86 pm) vs. Pt^{2+} ion (80 pm). Ir^{3+} shows an even larger shift, because it is triple positive leading to a positive charge of the whole complex.

For the calculation of the cooperativity with the presented concept, it is important to consider the same electronic excitation for all investigated substances. Therefore, we only focus on the π-π* transition described above, which is localized on the ligand, i.e. the highest π orbital of the ligand is involved in the HOMO or HOMO-1. Therefore, band analyses of the experimental spectra are mandatory. These analyses are also shown in Figure 5 for the series of the platinum(II) containing complexes (**4** and **7**) and the counterparts for our concept (**1** and **5**) as well as in the Supporting Information (Figures S38–S53).

The maxima of the bands with the lowest energy in the spectra ($\tilde{\nu}$) are analyzed concerning their cooperativity. Consequently, the general equation [Equation (1)] can be transformed to:

$$\tilde{\nu}_{AB} \neq \tilde{\nu}_A + \tilde{\nu}_B - \tilde{\nu}_{Ligand} \quad (2)$$

In order to use the equation in a clearer way, it is rewritten:

$$cooperativeeffect = \tilde{\nu}_{ce} = \tilde{\nu}_A + \tilde{\nu}_B - \tilde{\nu}_{AB} - \tilde{\nu}_{Ligand} \neq 0 \quad (3)$$

By comparing the obtained values, it is obvious that both the experimental and the calculated values are negative for all three series and in both solvents (*cf.* Table 2). A negative value means that the bathochromic shift of the binuclear species is smaller than the sum of the shifts of the mononuclear species. According to our definition, it can be stated that cooperativity is negative. In the experiment, the values in dichloromethane are less negative than in chloroform, which is confirmed by the calculated values. The solvent-dependence is particularly evident for complexes **3** and **4**, which show a smaller bathochromic shift in the more polar solvent dichloromethane. This smaller shift leads to a lower negative cooperativity.

Furthermore, it is apparent that platinum(II) leads to a larger negative cooperative effect than palladium(II). This can be explained by the higher effective nuclear charge of platinum(II) that influences the π-π* transition at the ligand and results in a larger bathochromic shift of **4**. In the case of iridium(III) the values are even larger, since the charge of the Ir^{3+} cation is higher than the charge of the Pt^{2+} cation. At this point, it should be noted that the resulting effects are calculated from four values which all have an uncertainty, both in the experiment and the TD-DFT calculations, but even the maximum error does not lead to a change in the magnitude and sign of the cooperativity. Furthermore, the investigated electronic π-π* transition, especially in the binuclear complexes partly include additional contributions of MLCTs, since the HOMO/HOMO-1 has contributions from metal-centered orbitals.

Table 1. Shift of the π-π* transition relative to the ligand in different solvents.

Substance	CH_2Cl_2 Δλ [nm]	$\Delta\tilde{\nu}$ [cm^{-1}]	$CHCl_3$ Δλ [nm]	$\Delta\tilde{\nu}$ [cm^{-1}]
1 (Ligand)	0	0	0	0
2 (Ir^+)	81	−4807	78	−3959
3 (Pd)	38	−2491	65	−6454
4 (Pt)	75	−4510	119	−7358
5 (Ir)	144	−7502	142	−9347
6 (IrPd)	195	−9245	201	−9644
7 (IrPt)	203	−9490	211	−7906
8 ($IrIr^+$)	175	−8600	157	−4614

Table 2. Comparison of the cooperative effects in the series of four complexes in dichloromethane and chloroform, experimental and calculated (TD-DFT/B3LYP-D3/def2-TZVP).

	Ir–Pd [5+3−6−1]	Ir–Pt [5+4−7−1]	Ir–Ir [5+2−8−1]
$\tilde{\nu}_{ce}$ [cm^{-1}] (CH_2Cl_2, exp.)	−748±505	−2522±505	−3708±506
$\tilde{\nu}_{ce}$ [cm^{-1}] (CH_2Cl_2, calc.)	−546	−2833	−5420
$\tilde{\nu}_{ce}$ [cm^{-1}] ($CHCl_3$, exp.)	−1970±493	−4168±491	−4067±496
$\tilde{\nu}_{ce}$ [cm^{-1}] ($CHCl_3$, calc.)	−1106	−3653	−5557

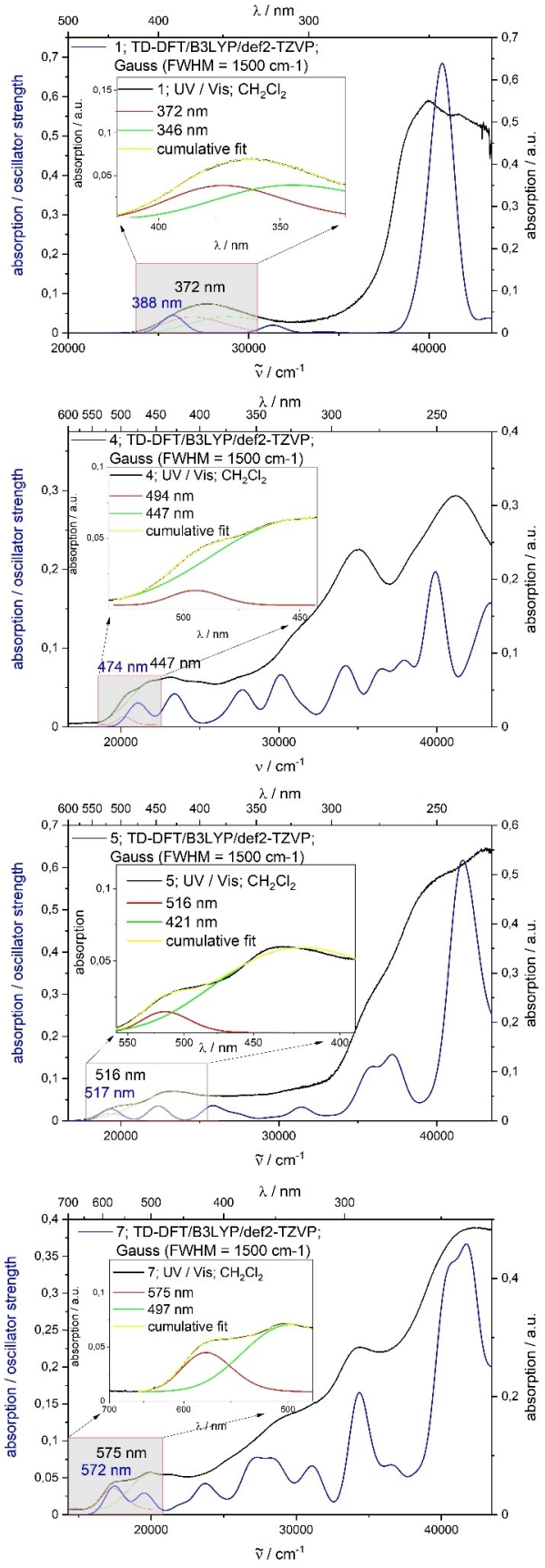

Figure 5. Experimental and calculated spectra of homologous series Ir–Pt (consisting of **1**, **4**, **5** and **7**) in CH_2Cl_2. The insets show a band analysis for the first excitations.

The negative cooperative effect can be interpreted in a way that both metals compete for the electron density in the ligand, which causes a weakening of the bonds between the transition metals and the ligand in the binuclear complexes compared to the mononuclear complexes. This is confirmed by considering the calculated metal-nitrogen and metal-carbon bond lengths (see Table S3). In the binuclear complexes, the bonds are slightly longer than in the mononuclear ones. As mentioned above, weakening of a metal-ligand bond by a second metal may lead to a decrease of the activation barrier of catalytic reaction. The presented systems can therefore be taken as examples of enthalpic cooperativity. The concept can also provide another aspect: The quantification of cooperativity offers the possibility to compare different binuclear metal complexes i.e. the absolute amount of the calculated value may also be interpreted as an indicator for quality of the combination of the metal ions in catalysis. In our case, it would predict that the homobimetallic combination of Ir^{3+}/Ir^{3+} is better than the heterobimetallic combinations Ir^{3+}/Pd^{2+} and Ir^{3+}/Pt^{2+}. The future aim is to provide the experimental evidence concerning the catalysis.

As already mentioned, the presented concept for the quantification of cooperative effects can be used for different properties. We therefore additionally applied it for the wavelengths of the luminescence. To perform this application, we have to be sure that we compare the same electronic transition.

As shown in Figure 6 for complex **7**, the luminescence wavelength depends on the selected excitation wavelength. At an excitation wavelength of 273 nm, an emission can be observed at approximately $\lambda_{EM} = 370$ nm in CH_2Cl_2, while at a higher wavelength of $\lambda_{EX} = 389$ nm the luminescence occurs at 450 to 480 nm. At even higher excitation wavelengths no luminescence can be detected. Since the above-mentioned π-π* transitions of the complexes **2**–**8** are in the range of 450 to 580 nm in the UV/Vis spectra, it is not possible that their luminescence is observed here. Consequently, the lowest visible luminescent transition must result from an electronic transition with higher energy. Because of the uncertainty of the nature of this transition, it is impossible to provide an appropriate

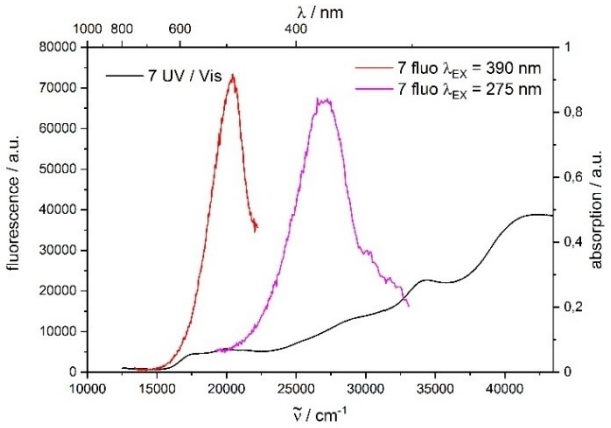

Figure 6. Absorption and emission spectra of IrPt-complex (**7**) in CH_2Cl_2 for two different excitation wavelengths.

theoretical description. Furthermore, the optimization of higher electronic states at the TD-DFT level often results in problems regarding conical intersections. Therefore, we are focusing on the experimental data. Here we analyze the luminescence transition with the lowest energy under the assumption that it is the same in all investigated substances.

For the pure ligand **1**, only one emission band at λ_{EM} = 460 nm in CH_2Cl_2 and λ_{EM} = 463 nm in $CHCl_3$ can be observed at every excitation wavelength between 400 nm and 250 nm. This band shows a mono-exponential decay with a lifetime of 4.7 ns in CH_2Cl_2 and 3.6 ns in $CHCl_3$, see Tables S4 and S5. All metal complexes show two luminescence wavelengths as a function of the excitation wavelength, they are summarized in Figures S13–S28 as well as in Tables S4 and S5. We used the energetically lower transition for our analysis.

Figure 7 shows the luminescence spectra for the series of palladium(II)/iridium(III) in $CHCl_3$. The other series are shown in the Supporting Information, Figures 54–59. It can be seen that the coordination of the metals also influences the position of the luminescence band. While the C,N-coordination of iridium(III) (in **5**) leads to a blue-shift of the luminescence relative to ligand **1**, the N,N-coordination of palladium(II) (**3**), platinum(II) (**4**) and iridium(III) (**2**) results in a red-shift. In the bimetallic complexes **6**, **7** and **8**, the red-shift is even more pronounced (by a factor of 2 to 3, see Table S6). From this we can conclude that cooperativity exists, since a pure additivity would predict a smaller red-shift or a smaller blue-shift for the bimetallic case (Table S6). Using the maxima of the bands for the same analysis as shown above, we can also quantify this cooperative effects at least with respect to the purely experimental data. Table 3 gives an overview of the obtained values. In CH_2Cl_2, the spectra of **2**, **4** and **5** show a dual luminescence due to a shoulder on the lower-energy flank. We have chosen the wavelength of this shoulder for our analysis to meet the condition of using the lowest energy transition.

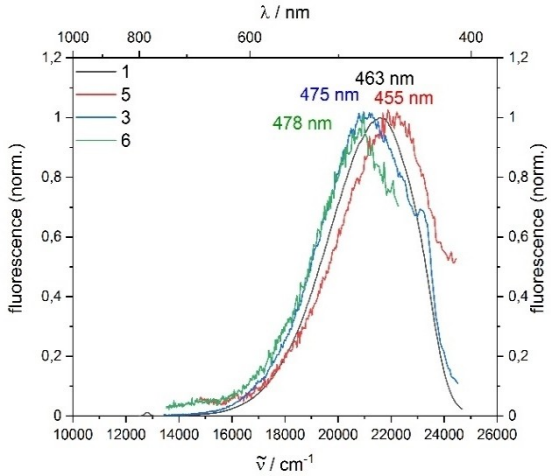

Figure 7. Series of the luminescence spectra of **1**, **3**, **5** and **6** at the excitation wavelength of 390 nm in $CHCl_3$.

Table 3. Comparison of the cooperative effects in the series of four complexes in dichloromethane and chloroform concerning their luminescence.

	Ir–Pd [**5**+**3**−**6**−**1**]	Ir–Pt [**5**+**4**−**7**−**1**]	Ir–Ir [**5**+**2**−**8**−**1**]
$\tilde{\nu}_{ce}$ [cm^{-1}] (CH_2Cl_2, exp.)	1000 ± 169	924 ± 159	1070 ± 167
$\tilde{\nu}_{ce}$ [cm^{-1}] ($CHCl_3$, exp.)	512 ± 123	510 ± 105	1089 ± 121

The analysis reveals a positive cooperative effect for all series and both solvents. Compared to the values obtained from the UV/Vis absorption, the luminescence values are smaller. For the series Ir–Pd and Ir–Pt, the cooperative effect in CH_2Cl_2 is almost twice the value as in $CHCl_3$, while for the Ir–Ir series, the values are similar for both solvents. This solvent-dependence could also be found for the values of the UV/Vis data. The difference between palladium(II), platinum(II) and iridium(III) is probably not significant. This analysis of luminescence data suffers from the comparison with theory but it should indicate that the general concept is also applicable to other (photo)physical properties.

Conclusion

The experimental data of UV/Vis (and fluorescence) spectra in different solvents as well as TD-DFT calculations are used in this manuscript to demonstrate the performance of the chosen concept to quantify cooperativity. By applying this strategy, the electronic excitations in these systems turn out to be significantly non-additive, in our case a negative cooperativity is observed. The magnitude of cooperativity depends on the combination of transition metals and the solvent. Since the investigated complexes are also useful in catalysis, the cooperativity might also give an indication or an explanation for the expected or observed catalytic reaction which may be accelerated by *e.g.* by weakening a metal-ligand bond. This has to be worked out in the future.

The formalism for quantifying cooperativity is not limited to UV/Vis data; it can be used as a universal scheme. Thus, it can be transferred to other properties and molecular systems as long as all components like the dinuclear, mononuclear complexes and the free ligand are synthetically available.

Experimental and Theoretical Methods

Quantum-chemical calculations

Input structures for the ligand and the complexes were generated by applying the universal force field (UFF)[19] implemented in the Avogadro program.[20] All structures are optimized using the Berny algorithm of Gaussian 09[21] with energies and gradients computed with Turbomole 7.4.[22] For this, the hybrid functional B3LYP with dispersion correction D3 is used.[23] For all atoms, the def2-TZVP basis set is applied, for the transition metals palladium, iridium and platinum, the def2-ecp is used. All structures are tested for being a minimum by frequency calculations, yielding no imaginary frequencies. Absorption spectra are calculated using TD-DFT with the same functional and basis set as used for the ground state calculations. For every structure, 50 excitations in the singlet manifold are

calculated. The resulting transitions are convolved with a Gaussian, simulating a full width at half maximum (FWHM) of 1500 cm^{-1}. Solvent effects are considered using the Conductor-like Screening Model (COSMO),[24] which is implemented in Turbomole. The used permitivities are 9.14 for dichloromethane and 4.806 for chloroform.

UV/Vis and Luminescence Spectroscopy

For all measurements, only spectroscopy grade solvents from Fluka were used. All measured solutions had a concentration in the range of $2*10^{-5}$ mol/L and were prepared with the common Schlenk technique under Argon atmosphere. The IRF (instrument response function) was determined via scattering of a diluted LUDOX® solution (TM-50 colloidal silica, 50 wt% suspension in water) solution (1/100), which has been purchased from Sigma-Aldrich.

The absorption spectra were recorded with a Perkin-Elmer Lambda 900 double beam UV/VIS/NIR spectrophotometer. Cylindrical quartz cuvettes with a path length of 1 cm were used. For detection of the emission a Horiba Jobin Yvon Fluorolog 3–22 τ and 1 cm × 1 cm quartz cuvettes were applied.[25]

Lifetime determination

The lifetime was determined with the time-correlated single-photon counting technique (TCSPC). Spectra were recorded with a DeltaFlex (Horiba Jobin Yvon) spectrometer.[26] The sample was excited with short light pulses of a NanoLED (273 nm, 389 nm) and the emission monochromator was set to the corresponding emission band for each complex. The precision photon counting is carried out with a PPT (picosecond photon counting) detection module, including a fast-rise PMT (photomultiplier tube) with an integral GHz timing preamplifier, a constant fraction discriminator and a regulated HV supply. Decay curves were analyzed with the software DAS-6, DataStation provided by Horiba Jobin Yvon. The average lifetimes were calculated using the amplitude average lifetime, which is defined by

$$\langle \tau \rangle_a = \sum_i a_i \tau_i \tag{4}$$

Acknowledgements

We thank the Collaborative Research Center SFB/TRR88 ("3MET") for financial support (projects B2 and C2). Mathias Klein und Gereon Niedner-Schatteburg are acknowledged for the measurements of the ESI-MS spectra (Figures S10–S12). Open access funding enabled and organized by Projekt DEAL.

Conflict of Interest

The authors declare no conflict of interest.

Keywords: cooperative effects · density functional calculations · fluorescence spectroscopy · heterometallic complexes · UV/Vis spectroscopy

[1] M. Böhmer, F. Kampert, T. Tsai Yuan Tan, G. Guisado-Barrios, E. Peris, F. E. Hahn, *Organometallics* **2018**, *37*, 4092–4099.
[2] A. Zavras, M. Kristić, P. Dugourd, V. Bonačić-Koutecký, R. A. J. O'Hair, *ChemCatChem* **2017**, *9*, 1298–1302.
[3] P. Buchwalter, J. Rosé, P. Braunstein, *Chem. Rev.* **2015**, *115*, 28–126.
[4] C. A. Hunter, H. L. Anderson, *Angew. Chem. Int. Ed.* **2009**, *48*, 7488–7499; *Angew. Chem.* **2009**, *121*, 7624–7636.
[5] C. Mück-Lichtenfeld, S. Grimme, *Dalton Trans.* **2012**, *41*, 9111–9118.
[6] L. Tebben, C. Mück-Lichtenfeld, G. Fernandez, S. Grimme, A. Studer, *Chem. Eur. J.* **2017**, *23*, 5864–5873.
[7] Y. Schmitt, K. Chevalier, F. Rupp, M. Becherer, A. Grün, A. M. Rijs, F. Walz, F. Breher, R. Diller, M. Gerhards, W. Klopper, *Phys. Chem. Chem. Phys.* **2014**, *16*, 8332–8338.
[8] M. Zimmer, F. Rupp, P. Singer, F. Walz, F. Breher, W. Klopper, R. Diller, M. Gerhards, *Phys. Chem. Chem. Phys.* **2015**, *17*, 14138–14144.
[9] J. Chmela, M. E. Harding, D. Matioszek, C. E. Anson, F. Breher, W. Klopper, *ChemPhysChem* **2016**, *17*, 37–45.
[10] G. Niedner-Schatteburg, in *Clusters – Contemporary Insight in Structure and Bonding* (Ed. S. Dehnen), Springer, Cham, **2017**.
[11] L. Taghizadeh Ghoochany, C. Kerner, S. Farsadpour, Y. Sun, F. Menges, G. Niedner-Schatteburg, W. R. Thiel, *Eur. J. Inorg. Chem.* **2013**, 4305–4317.
[12] A. Fizia, M. Gaffga, Y. Sun, G. Niedner-Schatteburg, W. R. Thiel, *Chem. Eur. J.* **2017**, *23*, 14563–14575.
[13] C. Kerner, J. P. Neu, M. Gaffga, J. Lang, B. Oelkers, Y. Sun, G. Niedner-Schatteburg, W. R. Thiel, *New J. Chem.* **2017**, *41*, 6995–7006.
[14] M. Leist, C. Kerner, L. Taghizadeh Ghoochany, S. Farsadpour, A. Fizia, J. P. Neu, F. Schön, Y. Sun, B. Oelkers, J. Lang, F. Menges, G. Niedner-Schatteburg, W. R. Thiel *J. Organomet. Chem.* **2018**, *863*, 30–43.
[15] F. Schön, M. Leist, A. Neuba, J. Lang, C. Braun, Y. Sun, G. Niedner-Schatteburg, S. Bräse, W. R. Thiel, *Chem. Commun.* **2017**, *53*, 12016–12019.
[16] S. M. Borisov, I. Klimant, *Anal. Chem.* **2007**, *79*, 7501–7509.
[17] W. Wu, W. Wu, S. Ji, H. Guo, J. Zhao, *Dalton Trans.* **2011**, *40*, 5953–5963.
[18] W. Wu, X. Wu, J. Zhao, M. Wu, *J. Mater. Chem. C* **2015**, *3*, 2291–2301.
[19] A. K. Rappe, C. J. Casewit, K. S. Colwell, W. A. Goddard, W. M. Skiff, *J. Am. Chem. Soc.* **1992**, *114*, 10024–10035.
[20] M. D. Hanwell, D. E. Curtis, D. C. Lonie, T. Vandermeersch, E. Zurek, G. R. Hutchison, *J. Cheminf.* **2012**, *4*, 17.
[21] M. J. Frisch, G. W. Trucks, H. B. Schlegel, G. E. Scuseria, M. A. Robb, J. R. Cheeseman, G. Scalmani, V. Barone, B. Mennucci, G. A. Petersson, H. Nakatsuji, M. Caricato, X. Li, H. P. Hratchian, A. F. Izmaylov, J. Bloino, G. Zheng, J. L. Sonnenberg, M. Hada, M. Ehara, K. Toyota, R. Fukuda, J. Hasegawa, M. Ishida, T. Nakajima, Y. Honda, O. Kitao, H. Nakai, T. Vreven, Montgomery Jr., J. A., J. E. Peralta, F. Ogliaro, M. J. Bearpark, J. Heyd, E. N. Brothers, K. N. Kudin, V. N. Staroverov, R. Kobayashi, J. Normand, K. Raghavachari, A. P. Rendell, J. C. Burant, S. S. Iyengar, J. Tomasi, M. Cossi, N. Rega, N. J. Millam, M. Klene, J. E. Knox, J. B. Cross, V. Bakken, C. Adamo, J. Jaramillo, R. Gomperts, R. E. Stratmann, O. Yazyev, A. J. Austin, R. Cammi, C. Pomelli, J. W. Ochterski, R. L. Martin, K. Morokuma, V. G. Zakrzewski, G. A. Voth, P. Salvador, J. J. Dannenberg, S. Dapprich, A. D. Daniels, Ö. Farkas, J. B. Foresman, J. V. Ortiz, J. Cioslowski, D. J. Fox, "Gaussian 09." Gaussian, Inc, Wallingford, CT, USA, Rev.D, **2009**.
[22] F. Furche, R. Ahlrichs, C. Hättig, W. Klopper, M. Sierka, F. Weigend, *Wiley Interdiscip. Rev.: Comput. Mol. Sci.* **2014**, *4*, 91–100.
[23] S. Grimme, J. Antony, S. Ehrlich, H. Krieg, *J. Chem. Phys.* **2010**, *132*, 154104.
[24] A. Schäfer, A. Klamt, D. Sattel, J. C. W. Lohrenz, F. Eckert, *Phys. Chem. Chem. Phys.* **2000**, *2*, 2187–2193.
[25] P. C. DeRose, E. A. Early, G. W. Kramer, *Rev. Sci. Instrum.* **2007**, *78*, 033107.
[26] D. J. S. Birch, G. Hungerford, D. McLoskey, K. Sagoo, P. Yip, in *Fluorescence in Industry*, pp. 103–133, Springer, Cham, **2019**.

Manuscript received: February 1, 2021
Revised manuscript received: March 17, 2021
Accepted manuscript online: March 26, 2021